This document is downloaded from DR-NTU, Nanyang Technological University Library, Singapore.

Title	Critical temperatures in thermocompression gold stud bonding
Author(s)	Zhang, G. G.; Ang, X. F.; Chen, Z.; Wong, Chee C.; Wei, J.
Citation	Zhang, G. G., Ang, X. F., Chen, Z., & Wong, C. C. & Wei, J. (2007). Critical temperatures in thermocompression gold stud bonding. Journal of Applied Physics, 102 (6).
Date	2007
URL	http://hdl.handle.net/10220/7735
Rights	© 2007 American Institute of Physics. This paper was published in Journal of Applied Physics and is made available as an electronic reprint (preprint) with permission of American Institute of Physics. The paper can be found at the following DOI: http://dx.doi.org/10.1063/1.2783974. One print or electronic copy may be made for personal use only. Systematic or multiple reproduction, distribution to multiple locations via electronic or other means, duplication of any material in this paper for a fee or for commercial purposes, or modification of the content of the paper is prohibited and is subject to penalties under law.

Critical temperatures in thermocompression gold stud bonding

G. G. Zhang, X. F. Ang,[a] Z. Chen, and C. C. Wong
School of Materials Science and Engineering, Nanyang Technological University, 50 Nanyang Avenue, Singapore 639798, Singapore

J. Wei
Singapore Institute of Manufacturing Technology, 71 Nanyang Drive, Singapore 638075, Singapore

(Received 15 June 2006; accepted 3 August 2007; published online 25 September 2007)

A study on temperature dependence in gold-gold (Au–Au) thermocompression bonding was performed. Gold studs were bonded to two kinds of surfaces—cofired gold on alumina and electroless nickel covered with immersion Au on silicon. A critical bonding temperature was observed for both substrates. No bonding occurs when the temperature is below this threshold value, whereas bond strength increases with bonding temperature beyond the threshold. This critical temperature can be related to the activation of organic films on the bonding surfaces. Under similar bonding conditions, the critical temperature is lower for a harder substrate than for a softer substrate, primarily because of larger interfacial shear stresses. This is supported by the observation on the interfacial shear stress distribution at the bonding interface based on finite element simulation models of substrates with different hardness. © *2007 American Institute of Physics*.
[DOI: 10.1063/1.2783974]

I. INTRODUCTION

Three-dimensional (3D) integration technology could potentially alleviate interconnection-related problems and enable high density and highly functionalized devices.[1,2] By using a 3D instead of a two-dimensional (2D) architecture, the maximum global interconnect length and the average global interconnect length both decrease by a factor equal to the square root of the number of dies stacked.[1] It has also been reported that the signal interconnect lines were much reduced in a 3D integrated chips (ICs) because the distance between each layer is in the order of 1–2 μm.[3] The fabrication of a 3D IC device is strongly dependent on five key technologies: (1) wafer thinning, (2) through-via, (3) wafer alignment, (4) bonding, and lastly (5) metallization. Precise alignment and stacking of thinned wafers using plated or filled through-vias are necessary for the development of 3D integration. Finally, buried interconnections with thin metallization layers formed on top of the buried vias and/or bonding between microbumps made of solder or metal such as gold and copper are used to provide both mechanical and electrical connections in a stacked chip. While each key technology contains its own limitations, the bonding between stacked layers is commonly considered to be the true bottleneck. There are a few bonding approaches. These different bonding schemes can be categorized into two common processes that have been applied in conventional chip-scale or wafer-level packaging techniques, namely, intermediate layer bonding such as soldering[4] and polymer glues,[5] or nonintermediate layer bonding such as Si (Ref. 6) and direct metal (copper-copper or gold-gold) bonding.[7] In the simplest case of a 3D interconnection where a flip chip is placed onto a chip, i.e., face to face interconnection of two dies, solder bumps were placed onto pads of single chips to form connections.[1] Although soldering offers high yield connections, it requires complex and often environmentally unsound processes. Poor reliability of solder connections formed is also known to occur under harsh conditions such as high thermal stress induced in the bumps.[8] Furthermore, solder joining is also not suitable for pitches less than 50 μm. The detrimental effect due to intermetallic growth is likely to be amplified in microjoints. Hence, to resolve the weaknesses of solder joints, alternative joining process employing adhesives are used. They are, however, limited by their lower reliability[9] due to moisture attacks and voids that result in poor mechanical properties and relatively poorer joint strength.[10] Direct metal bonding, on the other hand, is a method of joining two metal surfaces under ambient conditions without an intermediate layer (glue) in between. It is a promising candidate for solving all the above problems. Metallurgical joints are highly reliable and can be applied to fine pitch interconnections with little or no melting during the process. One of the most common materials used is gold. Gold is especially preferred due to its excellent resistance to oxidation. As such, gold to gold bonding has been commonly used in IC connections such as flip chips[11] and wire bonding.[12] These bumps were usually formed by ball wire bonding and electroplating. Both gold and copper microbumps have since been employed as interconnects in three-dimensional integrated circuits.[7,13] Thermosonic and thermocompression bonding are popular processes for direct metal bonding. However, while the bonds formed might be initially strong, they can be severely weakened by thermal stresses.

Thermal effects such as thermomechanical stresses are one of the major concerns that determines the performance and cost of a 3D device. As further reduction in chip size and increase in power consumption result from high density cir-

[a]Author to whom correspondence should be addressed. Electronic mail: angx0004@ntu.edu.sg

 © 2007 American Institute of Physics

Downloaded 25 Sep 2007 to 155.69.42.33. Redistribution subject to AIP license or copyright, see http://jap.aip.org/jap/copyright.jsp

cuitry, thermal effects are exacerbated, eventually leading to poor device performance and shortened lifetimes.[2] Furthermore, the fragility of thinned wafers used in stacked device architectures set practical upper limits on the temperatures and pressures used in bonding. At some point where current bonding parameters can only be lowered due to material, design, and manufacturing constraints, there will be a practical limit to the number of device layers stacked or circuits incorporated with a single chip due to high thermal budget. Bonding methods using excessive thermal and mechanical load will then become an immediate stumbling block for 3D IC application. Therefore, while the idea of 3D chips is rising as one of the key solutions to future complex electronic devices, its potentially wide applications are likely to be limited by the relatively large thermomechanical stresses employed during highly loaded thermocompression bonding. To achieve direct metal bonding at lower temperature and pressure is clearly a highly desired goal. Towards this end, the role of both processing parameters needs to be better understood.

Despite numerous empirical studies carried out to determine the optimum bonding parameters, the basic bonding mechanism that includes the physics and the mechanics is still not well understood. Current understanding of the bonding mechanism revealed the need for plastic flow of joint material in order to remove organic contamination, thus exposing clean surface for intimate contact. Besides the evaluation on effects of surface contamination and cleaning prior bonding, Jellison[12] found an improvement in gold to gold strength if postheating at elevated temperature is imposed at elevated temperature of 250 °C and postulates that the thermal input is to facilitate removal of contamination. From here, it is obvious that the knowledge of the bonding mechanism is essential in order to determine the necessary amount of energy to facilitate material flow to keep the surfaces in contact, which, in turn, are significantly determined by external parameters of thermocompression bonding.

Hence, in this paper we focus on explaining the role of temperature in the formation of a metallic bond in thermocompression bonding. Gold studs were bonded onto two kinds of substrates—cofired gold layer on alumina and electroless nickel covered with a thin layer of immersion gold on silicon. We found a critical temperature below which no bonding can take place. It is believed that this critical temperature represents the minimum amount of heat required to just sufficiently remove organic contaminants completely for bonding to take place.

II. EXPERIMENTS

A. Materials

The bonding was conducted using 5×5 mm^2 die with 20 gold bumps, as shown in Fig. 1(a). The aluminum pads' pitch was 250 μm. The gold bumps were formed using a wire bonder with 25 μm gold wire. The bump size ranged from 75 to 80 μm in diameter and from 47 to 50 μm in height [Fig. 1(b)]. Two kinds of substrates were used for the bonding: one was 1 mm thick 96.5% alumina with 10 μm thick gold layer produced by paste printing and cofiring (sintering) in a furnace at about 900 °C to form multilayer ceramic structure. Organic residues present after firing were removed after cleaning. The other was 0.5 mm thick silicon with metal films deposited sequentially: first, a 80 nm TiW adhesion layer, then 100 nm sputtered Cu and 5 μm electroless plated Ni [16 at. % phosphorous (P) in NiP], and followed by 50 nm immersion gold. The mechanical properties of electroless plating nickel are very different from that of gold. The two materials were used so that the results would be far apart enough to study the effect of the substrate.

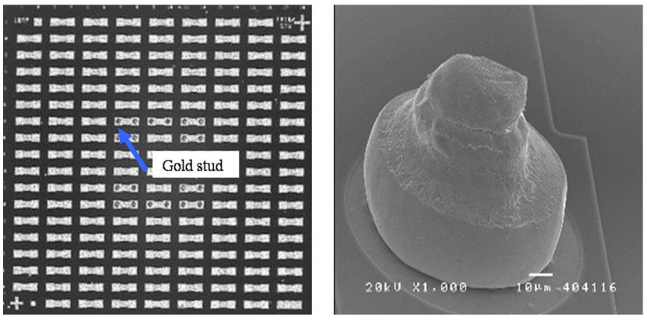

FIG. 1. (Color online) FA10 full array die with 20 pull-off bumps. (a) FA10 die; (b) Au stud bump.

B. Experimental procedures

The thermocompression bonding process was done using Panasert FCB-M flip chip bonder. The bonding procedure begins with the substrate sitting on a heated stage. A vacuum holds the substrate. When the stage is heated to a specified temperature, the chip is picked by the bonding tool with vacuum and is brought into contact with the substrate. After the bonding force has reached a certain level, the pickup tool is heated to predetermined temperature and maintained for some time to complete the process. The samples are left on the heated stage long enough to eliminate any effects of temperature transients. Even though two different substrates are being used, their small thermal masses ensure that the actual substrate temperature can be approximated by the stage temperature in both cases, with an estimated difference of only about 0.05 °C between the two substrates. Bonding quality was evaluated by die shear test, which was performed at a rate of 0.2 mm/s. The joint strength was expressed as the average shear force per bump. The fracture surfaces were examined by scanning electron microscopy (SEM) and optical microscopy.

C. Bonding modeling

Based on the joint interface mechanics resulting from joint bump compression, a finite element model was created to compare the bonding on different substrates. The model studies the variation of the interfacial stress distribution along the radial bonding surfaces. The 2D finite element model (plane42) with axisymmetrical condition assumed was built using ANSYS 8.0 shown in Fig. 2. Since there is an axis of symmetry at the center of bump and the substrate, only one-half of the cross section was used for the model. Physical properties such as elastic Young's modulus, Poisson ratio, and yield strength of gold were used as inputs for material

Downloaded 25 Sep 2007 to 155.69.42.33. Redistribution subject to AIP license or copyright, see http://jap.aip.org/jap/copyright.jsp

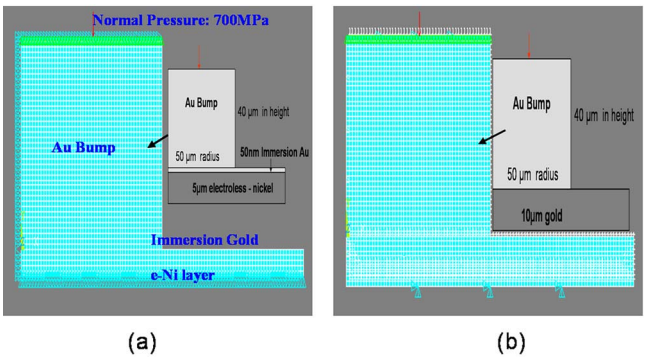

FIG. 2. (Color online) Finite element grid with boundary conditions. (a) Gold bump on immersion gold with underlying *e*-Ni layer (harder); (b) gold bump on thick gold layer (soft).

properties of the model. Rate independent plasticity material properties based on bilinear isotropic hardening were included to accommodate for large strain and deformation that usually occurs in metals such as gold. The physical properties of gold paste and electroless nickel layer, respectively (yield strength and young's modulus are determined by nanoindentation), are shown in Table I. It was also assumed that there is no relative motion between the bump and the substrate, since any force sufficient to deform the bump will cause "sticking" between the two contacting surfaces.[14] Material properties for printed gold paste are used for both models to investigate the effect of a harder underlying layer on the interfacial stress distribution after compression. Surface load which implies a distributed load over the top surface of the bump were applied in the model. The bonding temperature in actual thermocompression bonding is neglected in this simulation. For the purpose of comparison, the exact stress is not required.

III. RESULTS AND DISCUSSION

A. Critical temperature

Previous studies on gold-gold thermocompression bonding explored a wide range of bonding temperature and its effect on the joint strength formed, depending on its configuration and other key experimental parameters such as pressure and time. For example, gold-plated leads were bonded to gold metallization at temperatures between 270 and 620 °C to evaluate the corresponding bonding time needed for bond completion. On the other hand, gold ball bonding[15] was investigated at a heated capillary temperature ranging from 150 to 200 °C and substrate temperature above 300 °C. It is understood that, with the effect of substrate and chip heating, the pressure and the amount of bonding time influence the creation of a gold-gold metallurgical bond and its strength. An increase in bonding temperature, pressure,

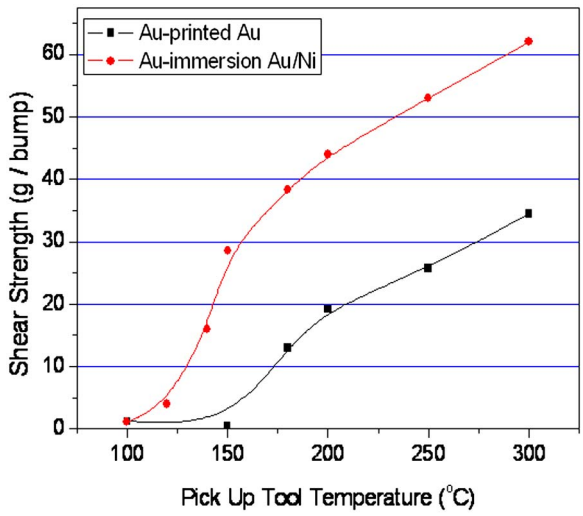

FIG. 3. (Color online) The effect of pickup tool temperature on shear strength of joints at bonding pressure of 500 g per bump.

and time was generally found to increase the shear strength of gold-gold joint.[12,16] However, the true role of temperature in aiding bonding has not been mentioned. In this report, a lower range of bonding temperature was explored to evaluate the minimum temperature required to form a gold-gold bond and a postulation of the role of temperature was made.

In the thermocompression bonding of gold stud to 10 μm gold layer on alumina (Au-printed Au) and on immersion gold on electroless plated nickel (Au-immersion Au/Ni), respectively, the bonding load was 500 g per bump and the bonding time was 10 s. The influence of pickup tool temperature (T_{tool}) was studied from 100 to 300 °C, while keeping the stage temperature (T_{stage}) fixed at 150 °C. The result is shown in Fig. 3, which indicates the existence of a threshold T_{tool} for both substrates. Below this critical value (150 °C in the case for Au-printed Au joint and 120 °C for Au-immersion Au/Ni joint), there is nearly no joining as the joint strength is near zero. Above this critical point, small increase of temperature produces large improvement in joint strength. In other words, the critical T_{tool} is the transition from "no bonding" condition to "bonding" condition. With the further increase of temperature, the joint strength increases steadily. Evidence that bonding does not take place below the critical T_{tool} can also be seen in the cross sectional SEM images of Au-printed Au joints, as shown in Fig. 4. At the T_{tool} of 100 °C, large unbonded area was observed between the gold stud and gold layer. Such unbonded area disappeared at a higher temperature of 180 °C.

In such thermocompression bonding process, it is the interfacial temperature (T_{inter}) that controls the bonding quality. The existence of critical T_{inter} is exhibited through thresh-

TABLE I. Mechanical properties of gold and electroless nickel.

Materials	Young's modulus (GPa)	Poisson ratio	Yield strength (MPa)	Tangent modulus (GPa)
Gold paste	70	0.42	200	1.1
Electroless nickel layer	199	0.312	1500	1.2

Downloaded 25 Sep 2007 to 155.69.42.33. Redistribution subject to AIP license or copyright, see http://jap.aip.org/jap/copyright.jsp

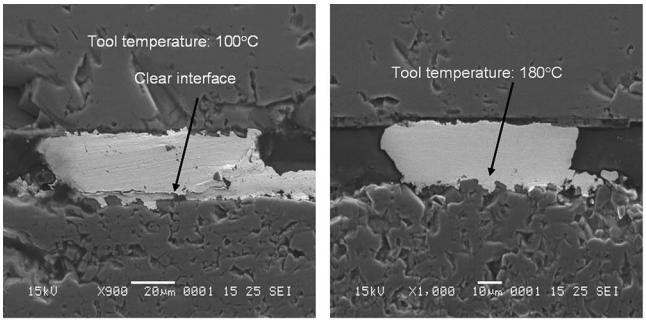

FIG. 4. Cross section SEM images of Au–Au joints on alumina substrate at different bonding temperatures.

old T_{tool} in the above investigation. T_{inter} depends on both T_{tool} and T_{stage}. Thus, with higher T_{stage}, lower critical T_{tool} is needed to produce certain critical T_{inter} for the bonding and vice versa. This indicates that the change of T_{stage} would result in the shift of threshold T_{tool}. To study the effect of T_{stage} on critical T_{tool}, bonding was carried out with lower T_{stage} of 100 °C. The result of this is shown in Fig. 5, together with that of 150 °C for comparison. When T_{stage} is decreased to 100 °C, the critical T_{tool} shifted to higher value (180 °C). At T_{tool} above threshold, the joints are always weaker when bonded with lower T_{stage} because the net T_{inter} is lower. This indicates that higher T_{stage} can be used to lower critical T_{tool}, so as to achieve satisfactory bonding with minimum damage to the devices.

While bonding time is also known as a contributing factor in influencing the bondability of metal joints, it is believed that it will only have an apparent effect on affecting the critical temperature if the bonding occurs in a very short time. Similarly, the effect of the obvious differences in surface morphology between Au-printed Au and Au-immersion Au/Ni substrates is postulated to have little influence in the critical temperature observed. While a thick printed gold layer is spatially rougher than a 50 nm immersion gold layer, the true contact surface between the stud surface and the substrate layer at submicron scale does not differ much for both types of surfaces.

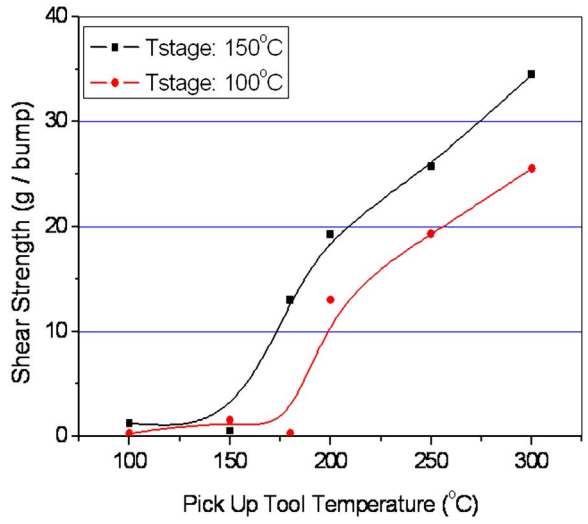

FIG. 5. (Color online) The effect of tool temperature at two stage temperatures using gold-gold on alumina.

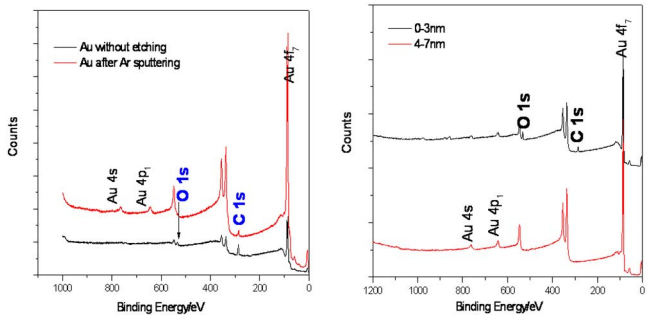

FIG. 6. (Color online) Surface chemical composition of gold (a) with/without Ar sputtering and (b) at different detection depths.

B. Interfacial chemical behavior

The existence of a critical temperature could be explained in terms of the minimum work needed to overcome a barrier film. It is widely known that films such as photoresist residues, oxides, etc., on bonding surfaces or even surface irregularities can impair the formation of a metallurgical bond.[17] Therefore, the requirement for producing a joint is that the two metal surfaces must be brought together within the operating range of interatomic attractive forces. If these two metal surfaces are atomically clean, flat, and smooth, a very strong bonding would be produced in the whole contact area when they are brought together. No external energy input is needed. Based on this theory, surface activated bonding (SAB) was developed for joining of metals, ceramics, and semiconductors at room temperature with small pressure applied.[18]

Another way to flatten the surfaces and break the bonding barrier films is to apply high pressure. Earlier studies on bonding had shown that perfect removal of such organic contaminant film or oxide film is impossible, thus necessitates the presence of plastic interfacial deformation to break down and disperse the barrier films.[12] Hence, the pressure applied produces a plastic metal flow along the bonding surface and helps to reduce the asperities. Surface oxide layers and contamination films can be disrupted, and "clean" metal on both surfaces thus comes into contact. The success of such methods depends critically on whether the barrier film could be broken. Gold does not form oxides. However, gold would be coated with adsorbed organic layers when exposed to air.[12] Such a layer is of high ductility and mobility. Even after an extensive deformation (for the bonding load of 500 g per bump, the pressure is about 700 MPa, much larger than the yield strength of gold, which is 200 MPa), there may still be a monolayer of water vapor or other gases between the two flattened gold surfaces which prevents bonding. This argument is supported by McGuire *et al.*[19] who found that even above a certain amount of bond strength achieved, the gold surface still contains a very thin layer of foreign materials with C and O as the major components.

A survey spectrum was collected on the Au-immersion Au/Ni silicon substrate using x-ray photoelectron spectroscopy (XPS) to determine the existence of a layer of organic contaminants on gold surface. From Fig. 6(a), the presence of the organic contaminant layer on gold surface was demonstrated. A comparison made between the compositional

Downloaded 25 Sep 2007 to 155.69.42.33. Redistribution subject to AIP license or copyright, see http://jap.aip.org/jap/copyright.jsp

spectrum for gold surface prior cleaning and gold surface after some cleaning using argon sputtering for 3 minutes revealed that there is an inherent layer of surface contaminants on gold that consists of carbon and oxygen as the major constituents. This is not surprising as it has been understood that for a real surface model, a layer of surface contaminants exists. However, after 3 min of argon sputtering, O 1*s* spectra disappeared and C 1*s* emission peak showed a significant drop in intensity as compared to that without cleaning. With the huge reduction in organic contaminants present, emission peaks from outer core shells, Au 4*s* and Au 4*p*, gradually emerged.

Besides that, a surface composition analysis done on the gold surface at different detection depths revealed that the thickness of the contamination layer is most likely to be less than 4 nm, evidenced by the chemical composition spectra at 0–3 and 4–7 nm detection depth, respectively, as shown in Fig. 6(b). Beyond 4 nm depth, no carbon and oxygen contents are present, as only sharp peaks due to gold are observed. The XPS spectra at depth below 4 nm showed high core level peaks for gold at 87.6 eV (Au $4f_7$) as well as for C 1*s* (285.6 eV) and O 1*s* (532.6 eV). These major components of surface contaminants are both absent in the chemical spectrum at above 4 nm depth.

Therefore, as explained previously, an amount of energy is thus needed to overcome the barriers which remain after mechanical deformation. One such mechanism is thermal desorption. Because the barriers are already very thin and could easily diffuse away, the activation energy is relatively low and could be supplied by moderate heating. The critical temperature is, thus, the point where the supplied thermal energy is sufficient to remove the deformed barrier film. When a sample surface contains a ductile contamination layer, bonding could not be achieved without sufficient thermal energy input, even if a sufficiently high pressure is applied and localized contact produced. This finding agrees with what was reported by Jellison, that bonding was highly temperature dependent when organic films were present on the gold surfaces.[12] He found that the shear strength of the thermocompression gold joints improved after UV cleaning was carried out on the gold surfaces. The extra cleaning step reduced the thickness of residual carbon layer to less than 1 Å but does not fully remove the inherent layer. Hence, the hypothesis of a critical temperature also explain the presence of a minimum temperature required for bond formation between gold found by Hu *et al.*[20] even when ultrasonic energy was applied.

In the case of gold stud bonding to a harder substrate, Au-immersion Au/Ni bonding also exhibits a critical T_{tool} in the bonding, as shown in Fig. 3. However, compared to Au-printed Au bonding, Au-immersion Au/Ni bonding has a lower critical T_{tool}. Under the same bonding condition, Au-printed Au samples did not bond at the temperature of 150 °C, while the joint strength of Au-immersion Au/Ni bonding is 28.5 g/bump. Since the electroless nickel surface was covered by a layer of immersion gold, the bonding itself is still gold to gold bonding, which, in all likelihood, will be contaminated by similar ductile organic surface layers as in the earlier case of Au–Au bonding. The interfacial chemical state could be considered the same for Au-immersion Au/Ni and Au-printed Au, thus explaining why a critical temperature is also observed. Therefore, it is believed that the different critical T_{tool} would be more likely caused by the different interfacial mechanics caused by the harder underlying metal layer which would be explained in the next section.

C. Influence of interfacial stress distribution

Critical temperature is caused by the existence of ductile contaminant layer and related to the thermal desorption of the deformed barrier film. With a larger deformation, a thinner barrier film is produced and thus a lower threshold temperature is needed. For contaminated surfaces, plastic deformation under normal loads (without tangential loads) is ineffective in contaminant disruption.[21] This is also evident in Ahmed and Svitak's study which found that the high normal stresses were not sufficient for bond formation, but rather, the tangential component of shear stress that could influence bond formation by aiding deformation of asperities.[22] It is generally agreed that the applied force is needed to facilitate material flow to achieve full interfacial contact, and, through lateral deformation or interfacial shear, barrier films are broken down for formation of metallic bonds.[23] To produce two metal surfaces that are "ready to be activated," sufficient interfacial shear stress is required to reduce the barrier film to a certain thickness. This understanding is further supported by Bay[24] who showed theoretically that the bond interface exposed for bonding is governed by the interfacial deformation behavior.

In the case of thermocompression bonding, the interfacial shear is dependent on both pressure and bonding materials' mechanical property. It can thus be postulated that, even with the same bonding parameters, the interfacial deformation of different material combinations would be different, and so does the critical temperature. To compare the interfacial shear stress between the bonding of gold bump to different hardness substrate, finite element (FE) analysis was carried out. Since the initial contact area between the two real surfaces is too small to be accurately represented by the FE models, the models created aim to capture the later stage where actual bonding occurs, as initial disparities were flattened and surface contact area increases with increasing load. While surface irregularities are expected on a real stud surface, random distribution of asperities across the entire surface is assumed such that the stress distribution observed in the finite element model represents bulk deformation behavior. Gold bumps to thin Au-printed Au/Ni layer and to thick Au-printed Au layer were selected. The simulated results are shown in Fig. 8. It could be seen that shear stress at the interface is much smaller when gold is bonded to softer substrate, such as gold, shown by the stress contours in Fig. 7.

As shown above by the simulation, in the point of interface deformation, bonding would be favored in harder substrate. Given the yield strength of gold bump, the simulated results extracted at the interface shown in Fig. 8 reveal that a larger degree of plastic deformation will be expected at the bonded interface for Au-printed Au/Ni model since the amount of stress induced is much larger than that of a softer

Downloaded 25 Sep 2007 to 155.69.42.33. Redistribution subject to AIP license or copyright, see http://jap.aip.org/jap/copyright.jsp

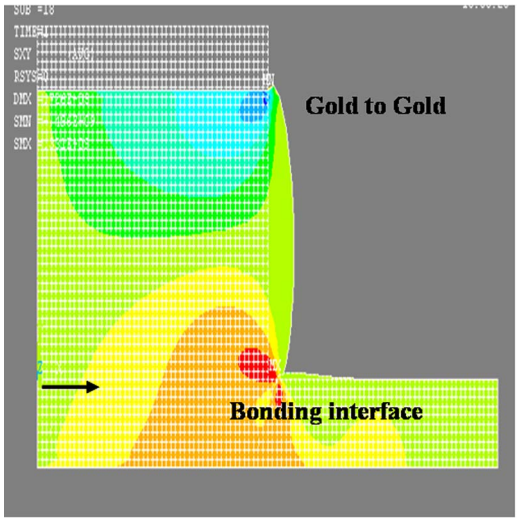

FIG. 7. (Color online) Typical stress contour (undeformed and deformed) diagram illustrating the shear stress distribution for gold bump-10 μm gold model.

substrate. There appears to be a less plastic flow in Au-printed Au model because the bump is more embedded into gold than into nickel. Thus, in Au-printed Au bonding, the residual contamination layer might be thicker than that in Au-immersion Au/Ni bonding under the same load. This reveals the need for more energy to break the layer which results in higher threshold bonding temperature. Such simulation results agree well with the experimental observation on the influence of substrate hardness on critical T_{tool} shown in Fig. 3.

D. Inward bonding behavior

Figure 8 shows the optical fractographs of Au-printed Au bonding at different pickup tool temperatures. When bonded at lower tool temperatures, such as 100 and 150 °C, all joints failed at the interface between the gold bump and the gold layer. The shear force was near zero, indicating no bonding.

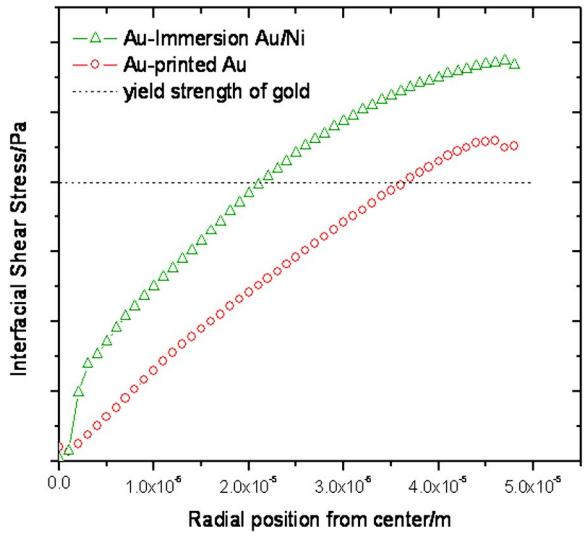

FIG. 8. (Color online) Simulated interfacial shear stress vs radial position of the gold joints.

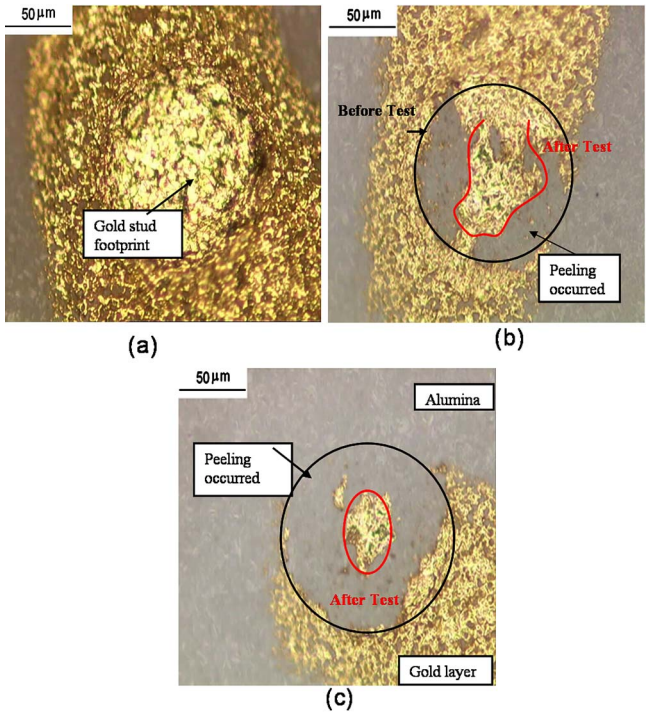

FIG. 9. (Color online) Optical fractographs of Au stud left on alumina substrate at different tool temperatures: (a) 150 °C, (b) 180 °C, and (c) 250 °C.

When tool temperature was raised over 150 °C, shear failures began to occur along the interface between gold layer and alumina substrate. In some areas, the gold layer was pulled off from substrate and adhered to gold bump. The shift of failure path from Au-printed Au interface to gold-alumina interface represents the improvement of joint strength and also the start of bonding. At that region the bonded interface is no longer the weakest point. It is at least stronger than the gold-alumina interface, whose adhesive strength is about 20 MPa, which is much lower than the metal bond strength. Thus, for the Au–Au bonding, it is reasonable to assume that there is no bonding if the joint fails along the bonded interface, and there is some degree of successful bonding if the failure is along the gold layer and alumina interface. Similar behavior was observed for Au-immersion Au/Ni samples. Comparing Figs. 9(a)–9(c), it could be seen that bonding first initiates at the outer region, and the bonding region grows inward with the increase of tool temperature. This corresponds with the simulated interfacial shear stress (Fig. 7). The shear stress is the largest in the outer region, where the contamination layer is disrupted more and the surface is easier to be activated for bonding. In the case of a cylindrical joint, the unbonded region should be the central region. Such peripheral bonding observed is not unique though. Wire thermocompression bonds[3,23] and even ultrasonic welds[25] were found to exhibit bonding at the periphery and no central bonding. In this report, gold stud thermocompression bonds revealed similar behavior. In our subsequent report, a more detailed finite element analytical model will be explored to understand the influence of boundary conditions at the bonding interface which could explain the bond formation from the outer region of the bumps.

Downloaded 25 Sep 2007 to 155.69.42.33. Redistribution subject to AIP license or copyright, see http://jap.aip.org/jap/copyright.jsp

IV. CONCLUSIONS

Based on the above results, the following conclusions are reached:

(1) There is a critical bonding temperature for thermocompression bonding. No bonding happens when temperature is below this threshold value. Such critical temperature is related to the activation of deformed organic films on the gold surfaces.
(2) The critical temperature required is reduced if in the presence of higher interfacial shear. This means that, under similar bonding conditions, the threshold temperature is lower for harder substrate than for softer substrate.

ACKNOWLEDGMENTS

We wish to acknowledge Ms. Lu Haijing, Mr. Cheng Chek Kweng, Tan Yang Kuang, Lai Foo Khuen, and Mohaime Bin Mohahidin for their experimental assistance.

[1]J. Baliga, IEEE Spectrum **41**, 43 (2004).
[2]K. Banerjee, S. J. Souri, P. Kapur, and K. C. Saraswat, Proc. IEEE **89**, 602 (2001).
[3]Y. Akasaka, Proc. IEEE **74**, 1703 (1986).
[4]A. Klumpp, R. Merkel, R. Wieland, and P. Ramm, Proceedings of the 53rd Electronic Components and Technology Conference, 2003, pp. 1080–1083.
[5]J. Q. Lu, Y. Kwon, R. P. Kraft, R. J. Gutmann, J. F. McDonald, and T. S. Gale, Proceedings of the IEEE International Interconnect Technology Conference, 2001, pp. 219–221; S. K. Kim and S. Tiwari, Integrated Circuit Design and Technology, 2005, pp. 183–186.
[6]R. Islam, C. Brubaker, P. Lindner, and C. Schaefer, Proceedings of the Advanced Semiconductor Manufacturing 2002 IEEE/SEMI Conference and Workshop, 2002, pp. 212–217.
[7]K. Tanida, M. Umemoto, Y. Tomita, M. Tago, Y. Nemoto, T. Ando, and K. Takahashi, Proceedings of the 53rd Electronic Components and Technology Conference, 2003, pp. 1084–1089.
[8]J. Simon and H. Reichl, Proceedings of the 50th Electronic Components and Technology Conference, 2000, pp. 81–86.
[9]A. O. Ogunjimi, O. Boyle, D. C. Whalley, and D. J. Williams, J. Electron. Manuf. **2**, 109 (1992).
[10]J. C. Jagt, IEEE Trans. Compon., Packag. Manuf. Technol., Part A **21**, 215 (1998).
[11]J. Jordan, Proceedings of the 27th Annual IEEE/CPMT/SEMI International Electronics Manufacturing Technology Symposium, 2002, pp. 110–114.
[12]J. L. Jellison, IEEE Trans. Parts, Hybrids, Packag. **11**, 206 (1975).
[13]R. Tadepalli and C. V. Thompson, Proceedings of the IEEE International Interconnect Technology Conference, 2003, pp. 36–38.
[14]T. S. McLauren and Y.-C. Lee, IEEE Trans. Adv. Packag. **23**, 652 (2000).
[15]H. Ramsey, Solid State Technol. **16**, 43 (1973).
[16]J. Jellison, IEEE Trans. Parts, Hybrids, Packag. **13**, 132 (1977).
[17]K. C. Joshi, Weld. J. (Miami, FL, U.S.) **50**, 840 (1971).
[18]T. Akatsu, N. Hosoda, and T. Suga, J. Mater. Sci. **34**, 4133 (1999).
[19]G. E. McGuire, J. V. Jones, and H. J. Dowell, Thin Solid Films **45**, 59 (1977).
[20]S. J. Hu, G. E. Lim, T. L. Lim, and K. P. Foong, IEEE Trans. Compon., Hybrids, Manuf. Technol. **14**, 855 (1991).
[21]R. Cuthrell and D. Tipping, IEEE Trans. Parts, Hybrids, Packag. **10**, 4 (1974).
[22]N. Ahmed and J. J. Svitak, Solid State Technol. **18**, 25 (1975).
[23]Y. Takahashi, S. Shibamoto, and K. Inoue, IEEE Trans. Compon., Packag. Manuf. Technol., Part A **19**, 213 (1996).
[24]N. Bay, Proc. Joining Met.: Pract. and Perform. **2**, 47 (1981).
[25]G. Harman and J. Albers, IEEE Trans. Parts, Hybrids, Packag. **13**, 406 (1977).

Downloaded 25 Sep 2007 to 155.69.42.33. Redistribution subject to AIP license or copyright, see http://jap.aip.org/jap/copyright.jsp